

## Dissociative Electron Attachment to Formamide: Direct and Indirect Pathways from Resonant Intermediates

T. P. M. Goumans,<sup>†</sup> F. A. Gianturco,<sup>\*,‡</sup> F. Sebastianelli,<sup>‡</sup> I. Baccarelli,<sup>§</sup> and J. L. Rivail<sup>||</sup>

*Department of Chemistry, University College London, 20 Gordon Street, London WC1H 0AJ, United Kingdom, Department of Chemistry and CNISM, University of Rome La Sapienza, Piazzale A. Moro 5, 00185 Rome, Italy SuperComputing Center CASPUR, via dei Tizii 6, 00185 Rome, Italy, and Laboratoire de Chimie Theorique, Université Henri Poincare, F54506 Vandoeuvre-les-Nancy, France*

Received September 9, 2008

**Abstract:** Dissociative electron attachment (DEA) to formamide (HCONH<sub>2</sub>), the smallest molecule with a peptide bond, is investigated with electron-molecule scattering calculations. At the equilibrium geometry we identify two resonances of A'' and A' symmetry at 3.77 and 14.90 eV, respectively. To further assess potential bond-breaking pathways for the transient negative ions (TNIs), the behavior of the resonances upon bond stretching of the C–H and C–N bond is investigated. While along the C–H dissociation coordinate neither resonance changes significantly, we find instead that both resonances are stabilized upon stretching the peptide C–N bond, with their resonance energy and width coming down rapidly, most strongly so for the A' resonance. The A' resonance is thus seen to disappear when the C–N bond is stretched for more than 1 Å, where it presumably smoothly connects to a bound anion state, a direct DEA pathway for the A' TNI to yield NH<sub>2</sub><sup>−</sup> and HCO. The A'' resonance is found instead not to be purely dissociative along the C–N coordinate but to evolve into forming a low-lying resonance on the NH<sub>2</sub> fragment. Furthermore, symmetry considerations dictate here that the incoming electron attaches itself to an orbital of A' symmetry of the NH<sub>2</sub><sup>−</sup> and HCO asymptotic fragments. Therefore, DEA from the A'' TNI has to occur via a symmetry-breaking, nonadiabatic curve crossing which connects to the purely dissociative A' metastable anionic state that is coming down in energy as the bond stretching occurs.

### 1. Introduction

The chemistry of low-energy electrons (LEEs) is currently actively investigated in view of its important role in radiation-induced damage to biomolecules<sup>1–14</sup> and in the processing of interstellar ices by cosmic rays.<sup>15–23</sup> The primary ionizing events are known to generate large amount of secondary electrons in the range of 0–20 eV<sup>24</sup> which can then resonantly attach themselves to molecular

targets and yield formation of transient negative ions (TNIs). The energized TNI, in turn, could either evolve by autodetaching the extra electron or could dispose of the excess energy within its molecular framework, a path which may ultimately lead to rupture of a chemical bond within the target: this process, yielding a stable anion and a radical fragment, is known as dissociative electron attachment (DEA). Here we study the resonances of formamide and its potential DEA pathways by using electron-molecule quantum scattering calculations. With similar methods, DEA processes in glycine,<sup>11</sup> uracil,<sup>3</sup> and formic acid<sup>4</sup> have been studied, while quantum dynamics coupled to quantum chemistry calculations have been used to study DEA in the sugar-DNA backbone.<sup>5</sup>

\* Corresponding author e-mail: fa.gianturco@caspur.it.

<sup>†</sup> University College London.

<sup>‡</sup> University of Rome La Sapienza.

<sup>§</sup> SuperComputing Center CASPUR.

<sup>||</sup> Université Henri Poincare.

Formamide is the smallest molecule with a peptide bond and has two resonance structures that give the C–N bond partial double bond character with a planarized nitrogen atom.<sup>25,26</sup> Formamide is observed in the interstellar medium, in star-forming regions<sup>27–31</sup> and in the comet Hale-Bopp<sup>32</sup> and has been suggested as a potential biological precursor because it forms nucleobases in the presence of oxides when UV-irradiated<sup>33</sup> or heated.<sup>34</sup> The processing of pure thin-film formamide ices has also been studied with low-energy electrons<sup>35</sup> and keV protons.<sup>36</sup> From anion-desorption studies of thin films of 1d-formamide on platinum Cloutier et al. conclude that  $\text{H}^-$  dissociates from the  $\text{NH}_2$ -group from a core-excited resonance (two-particle one-hole state) at  $\sim 8$  eV<sup>35</sup> but have not studied how the ice itself is processed. Brucato et al. report the formation of CO,  $\text{CO}_2$ ,  $\text{N}_2\text{O}$ , HNC, and  $\text{NH}_4^+\text{OCN}^-$  from irradiation of thin films of formamide on a silicon substrate with 200 keV protons,<sup>36</sup> which presumably results from the interaction of secondary low-energy electrons with the solid formamide.

Here we study the behavior of shape-resonances in gaseous formamide upon the stretching of the H–N, C–H, and C–N bonds to identify potential dissociative electron attachment pathways in the title molecule and to unravel possible energy deposition mechanisms.

## 2. The Computational Approach

The molecular quantum dynamical method we use in this study has been described in much detail previously;<sup>37–39</sup> therefore we give here only a short outline of it. The elastic electron-molecule scattering process is described within the fixed-nuclei approximation,<sup>38</sup> and the antisymmetrized scattering (electron + molecule) wave function is expanded from the Hartree–Fock (HF) orbitals of the neutral ground-state species, where the N electrons of the molecule target maintain their ground-state configuration during the scattering process, i.e. no core-excited resonances are considered. The scattering equations, orbitals, and potentials are expanded in a set of symmetry-adapted angular functions around the center of mass<sup>38,39</sup> and over a numerical radial grid out to the asymptotic region. The electron-molecule interaction potential is modeled by replacing the exact nonlocal exchange potential by an energy-dependent local potential, the Hara free-electron gas exchange,<sup>40</sup> and the correlation potential by the Perdew–Zunger potential.<sup>41</sup> Inclusion of a long-range polarization term changed very little the resonance results at the equilibrium geometry of formamide (see section 3.1). This is an expected behavior<sup>11</sup> since such transient state formations are clearly dominated by short-range correlation effects, and even more so when molecules with permanent dipole moments are considered. We can thus simplify the modeling of the interaction potential by neglecting the long-range polarization term.

Geometry optimizations and the potential energies of the neutral species along the bond-stretching coordinates have been calculated at the B3LYP/6–311+G\*\* level with Gaussian03,<sup>42</sup> while the HF/6–311+G\*\* orbitals are used for the scattering calculations. Elastic cross-sections and poles of the S-matrix have been calculated within  $A'$  and  $A''$  symmetry with the ePolyScat program,<sup>43</sup> at the equilibrium

geometry and at geometries where one of the bonds was stretched while all other bond lengths and angles have been held fixed, thus providing a pseudo-one-dimensional picture of the multidimensional Intramolecular Vibrational Redistribution (IVR) process as triggered by the resonant electron dynamics. For the S-matrix calculations we expanded the wave function with a maximum angular momentum value of 50, and a maximum of 14 partial waves was used for the scattering electron expansion within the piecewise diabatic representation. Increasing either values of the maximum angular momentum had no significant effect on the final results.

## 3. Scattering Results

**3.1. Equilibrium Geometry.** By searching for poles of the S-matrix in the complex plane, we find that, at the equilibrium geometry, two shape-resonances are deemed to be physically realistic, one for each symmetry. The  $A'$  resonance is at 14.90 eV and is very broad (with a hwhm of 2.08 eV), while the lower-lying  $A''$  resonance (3.77 eV) is much narrower (hwhm 0.52 eV). As in ref 11, also in the present case we checked the validity of our assumption concerning the negligibility of the long-range polarizability effects on the resonances' parameters. Hence, we repeated the calculations for the  $A''$  resonance at the equilibrium geometry by including the long-range part of the electron-molecule interaction. The spherical polarizability of the formamide employed in our calculations (25.30 Bohr<sup>3</sup>) was calculated at the same level of theory used to describe the ground-state of the neutral target (i.e., B3LYP/6311+G\*\*) and produced a value for the position of the  $\pi^*$  resonance shifted to higher energies by 0.008 eV. Such negligible shift confirms, once again, the validity of our assumption regarding the nature of the scattering potential which is responsible of the formation of transient anions. Hence, all the calculations at different nuclear geometries, discussed in the following section, do not include the long-range polarization interaction.

Our calculated  $A''$  resonance is almost 2 eV higher in energy than the one resonant feature determined by electron transmission spectroscopy (2.05 eV, fwhm 0.82 eV).<sup>44</sup> This discrepancy is most likely due to uncertainties in the measurements as well as inaccuracies in our calculations (fixed-nuclei approximation, model exchange interaction, localized correlation effects). Analysis of the piecewise adiabatic potential shows that the incoming electron is trapped by an  $l = 2$  centrifugal barrier in the  $A''$  resonance and is therefore classified as a d  $\pi$ -resonance. The resonant wave function (depicted in Figure 1) has a nodal plane between the C–N and C–H bonds, which suggest possible cleavage of these bonds as a potential dissociative electron attachment pathway.<sup>37</sup> Because Cloutier et al. observe  $\text{H}^-$  fragments from the  $\text{NH}_2$  group upon low-energy electron impact, we also consider N–H rupture, even though this process was there surmised to stem from a core-excited resonance without any further support for its occurrence and could also be heavily influenced by the metal substrate as well as other solid-state effects.<sup>35</sup> The corresponding spatial depiction of the broader

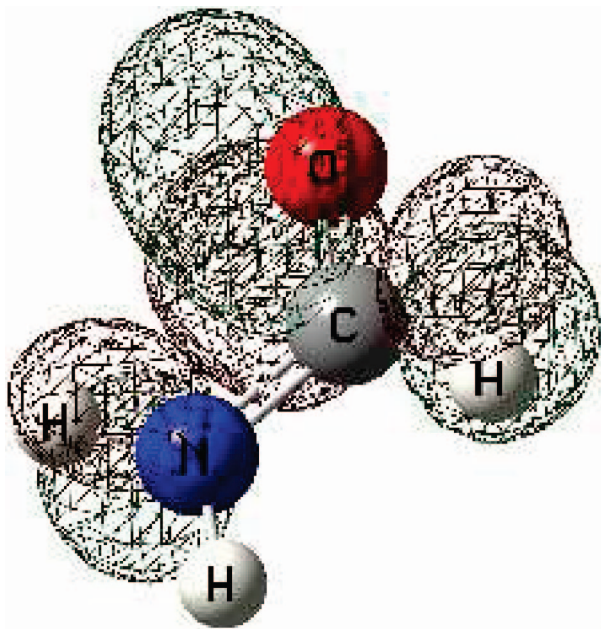


**Figure 1.** Mesh representation of A'' resonant wave function at the formamide equilibrium geometry.



**Figure 2.** Mesh representation of A' resonant wave function at the formamide equilibrium geometry.

A' resonance at higher energies (around 14 eV) is reported in Figure 2. We see there again the presence of an antibonding plane across the C–N bond and the additional presence of extra-electron densities above and below the C and the N atoms.

**3.2. Stretching of the C–H and N–H Bonds.** We carried out additional calculations, not reported here for the sake of brevity, which clearly showed that neither of the shape resonances changes much its location and width when either of the N–H bonds is stretched. More precisely, both resonances move slightly higher in energy, which excludes N–H bond stretching as a favorable pathway for transferring the excess energy of the TNI into the nuclear network. These results are in agreement with the proposal that the resonance at 8 eV giving rise to DEA by N–H bond rupture is not originating from a shape resonance but probably from some

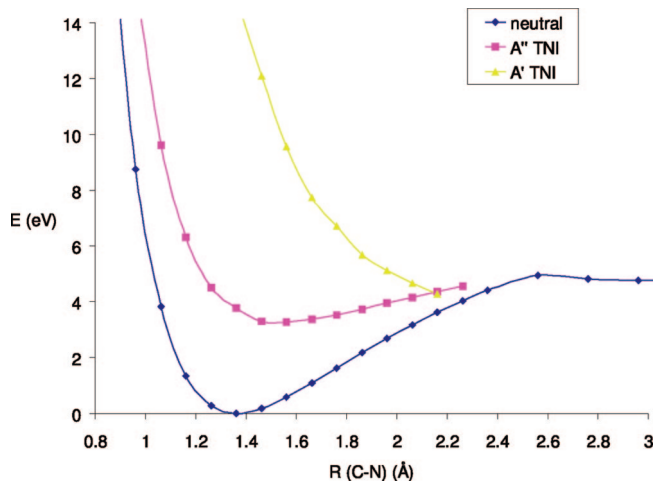


**Figure 3.** Electronic energy changes of formamide for the neutral and the two TNIs resonant states along the C–N stretching coordinate.

other mechanism.<sup>35</sup> On the other hand, upon stretching of the C–H bond both the A' and A'' resonances decrease very gradually in energy ( $\sim 0.1$  eV per  $0.1$  Å) when the bond is stretched beyond  $0.1$  Å. The energy is here with respect to the neutral species electronic energy taken to be the reference value. However, since the potential energy curve for the neutral species (see Figure 3) increases much more steeply than the actual resonance energy component decreases, C–H bond breaking is also surmised to be an unfavorable pathway for DEA processes which originate from the present shape resonances as intermediate anionic states: the overall anion electronic energy, in fact, increases as that bond is stretched.

**3.3. Stretching of the C–N Bonds.** Our further calculations clearly show, however, that both A' and A'' resonances are stabilized by the stretching of the central peptide bond. They quickly, and consistently, become lower in energy and more sharp (i.e., longer-lived) when the C–N bond is stretched from the equilibrium value of  $1.306$  Å, while compressing the C–N bond renders the resonances higher in energy and less stable, thereby making the electron-detachment path more likely to occur before energy redistribution within the nuclear network. To investigate the plausibility of C–N bond breaking as a potential pathway for DEA evolution of the TNIs, we followed the poles of the resonances until they disappeared, indicating formation of a stable anion. In Figure 3, we plot the energies of the neutral species and the A' and A'' TNIs along the C–N stretching coordinate. The energies of the TNIs at every geometry are calculated as the sum of the neutral species (at the B3LYP/6–311+G\*\* level) and the resonance energy:

$$E_{\text{TNI}}(R) = E_{\text{res}}(R) + E_{\text{neutral}}(R) - E(R_{\text{eq}}) \quad (1)$$

We see in the figure that the higher-energy A' resonance gets stabilized much more markedly as we stretch the bond than does the A'' resonance, a finding which makes the C–N stretching deformation a very efficient process for the transfer of the excess energy of the resonantly attached A' electron (14.9 eV) into the resulting fragments, although the short-lived TNI still has to compete with flux-losses into the electron autodetachment channel. When the C–N bond is



stretched by 0.8 Å out to 2.106 Å, the  $A'$  resonance (0.64 eV, hwhm 0.27 eV) has even become lower in energy than the  $A''$  resonance (0.74 eV, hwhm 0.02 eV). Further stretching leads to a disappearance of the  $A'$  resonance which indicates the formation of a stable anion. This feature is indicated in our calculations by the fact that the pole of the Scattering Matrix (S-matrix) locating the resonance now moves on the negative branch of the real energy axis and very close to it. Indeed we see in the figure that, when looking at the B3LYP/6-311+G\*\* level of calculations for the neutral species reported by diamonds in the figure, the anion of  $A'$  symmetry would proceed to become more stable than the neutral species when the C–N bond is stretched beyond 2.2 Å. We also find that the excess electron gets localized on the  $\text{NH}_2$  fragment, indicating  $\text{HCO} + \text{NH}_2^-$  as the likely DEA pathway of fragmentation. To obtain the actual crossing in Figure 3, however, we would need additional, separate calculations of the new bound (N+1) electron system within that range of geometries using conventional quantum chemistry codes, a test which is outside the scope of the present work and would not add to our analysis of the DEA processes as stabilizing mechanisms for resonant states.

One should further note here that, while the  $A''$  resonance gets also stabilized by C–N bond stretching, it does not disappear now into a bound state of the (N+1) electrons system for large C–N distances but rather evolves into a low-energy resonant state that localizes the excess electron onto the  $\text{NH}_2$  fragment. Because the excess electron has to attach itself to an orbital of  $A'$  symmetry in the asymptotic  $\text{HCO} + \text{NH}_2^-$  channel, we see that the  $A''$  TNI does not give rise to a direct DEA process: instead the existing TNI has to couple to the now nearby, fully dissociative  $A'$  potential curve by symmetry-breaking (e.g., pyramidalization of the  $\text{NH}_2$  group) in order to further proceed along a dissociative pathway. Our present calculations show that the two TNI curves are now crossing each other around 2.15 Å (Figure 3) at an energy of  $\sim 4.3$  eV above the ground-state energy of the neutral formamide. Therefore our dynamical modeling suggests here that for the 3.77 eV  $A''$  resonance to yield  $\text{HCO} + \text{NH}_2^-$  via an indirect DEA pathway it must cross the  $A'$  curve at a C–N distance of 2.15 Å, where the crossing will occur with an energy of  $\sim 0.5$  eV in excess of the resonance energy. Thus, the complex anion must therefore undergo a multidimensional IVR rearrangement before reaching the symmetry-breaking conical intersection that will yield the  $\text{NH}_2^-$  fragment.

#### 4. Discussion

Using realistic quantum scattering calculations, we have identified a direct (14.90 eV) and an indirect (3.77 eV) DEA pathways which could be followed by the fragmentation of gas phase formamide to yield  $\text{HCO} + \text{NH}_2^-$ . Our calculations also show that a dissociation of the H–C or the N–H bonds constitutes an unfavorable process for both TNIs observed in this system. The 3.77 eV shape resonance identified in our scattering calculations turns out to be located at a higher energy than the experimentally determined value of 2.05 eV (electron transmission spectroscopy),<sup>44</sup> which is an indication

that the true resonance is probably somewhere in between and that the indirect DEA pathway is also likely to be unfavored because of the sizable amount of excess energy needed to reach the seam where the  $A'$  and  $A''$  anion curves cross and can therefore optimally undergo nonadiabatic coupling.

Low-energy electron irradiation of thin films of solid 1d-formamide has established that mainly  $\text{H}^-$  anions desorb into the gas phase, resulting from N–H bond dissociation from a core-excited resonance around 8 eV.<sup>35</sup> However, that experiment would not detect any  $\text{NH}_2^-$  fragments that would have been formed by the shape-resonances around 3.8 and 15 eV and get trapped in the bulk since none of the products in the processed ice is experimentally determined. Likewise, our technique cannot be applied to identify possible core-excited resonances so we cannot uniquely establish whether or not the N–H formation is a plausible pathway for DEA processes originating from 8 eV low-energy electrons. Furthermore, since the solid matrix could considerably affect the position of the resonances by altering the permittivity and the geometries of the physisorbed species, and we have shown here that a small stretching of the C–N bond could already have a large effect on the position of the  $A'$  resonance (Figure 3), it is not at all clear that the feature around 8 eV seen experimentally actually occurs from molecules in their ground vibrational states and not from a lowering of the  $A'$  resonance due to some vibrational excitation effect.

Brucato et al. have identified several new molecules upon 200 keV proton irradiation of frozen formamide.<sup>36</sup> Since both products that appear to stem from C–N rupture ( $\text{CO}$ ,  $\text{CO}_2$ ) and from N–H rupture ( $\text{HNCO}$ ,  $\text{OCN}^-$ ) are observed, it could be argued that the secondary low-energy electrons generated in that process are actually producing both DEA processes. A detailed gas phase scattering study of formamide could shed more light on whether indeed fragmentation paths to  $\text{NH}_2^- + \text{HCO}$  take place from the high-energy (15 eV) and low-energy (3.7 eV) shape-resonances via the direct and indirect mechanisms which our calculations suggest. It is, in any event, of interest to have been able to argue purely from quantum calculations the likely presence of two possible, and distinct, molecular mechanisms that can lead to electron-induced fragmentation processes in gas phase formamide.

**Acknowledgment.** The work has been performed under the Project HPC-EUROPA++ project (project number: 211437), with the support of the European Community - Research Infrastructure Action of the FP7 “Coordination and support action” Programme. We also thank the CASPUR Supercomputing Consortium for computational support. The EPSRC is acknowledged for a postdoctoral fellowship for T.P.M.G. (EP/D500524), while the financial support of the University of Rome Research Committee is also acknowledged for the present research.

#### References

- (1) Boudaiffa, B.; Cloutier, P.; Hunting, D.; Huels, M. A.; Sanche, L. *Science* **2000**, 287, 1658–1660.

- (2) Sabin, J. R. Theoretical studies of the Interaction of Radiation with Biomolecules In *Advances in Quantum Chemistry*; Brändas, E., Sabin, J. R., Eds.; Elsevier: Amsterdam, 2007; Vol. 52, pp 1–3.
- (3) Gianturco, F. A.; Sebastianelli, F.; Lucchese, R. R.; Baccarelli, I.; Sanna, N. *J. Chem. Phys.* **2008**, *128*, 174302.
- (4) Rescigno, T. N.; Trevisan, C. S.; Orel, A. E. *Phys. Rev. Lett.* **2006**, *96*, 213201.
- (5) Simons, J. *Acc. Chem. Res.* **2006**, *39*, 772–779.
- (6) Balog, R.; Langer, J.; Gohlke, S.; Stano, M.; Abdoul-Carime, H.; Illenberger, E. *Int. J. Mass Spectrom.* **2004**, *233*, 267–291.
- (7) Sanche, L. *Mass Spectrom. Rev.* **2002**, *21*, 349–369.
- (8) Ingolfsson, O.; Weik, F.; Illenberger, E. *Int. J. Mass Spectrom. Ion Processes* **1996**, *155*, 1–68.
- (9) Sanche, L. *Eur. Phys. J. D* **2005**, *35*, 367–390.
- (10) Baccarelli, I.; Gianturco, F. A.; Grandi, A.; Sanna, N.; Lucchese, R. R.; Bald, I.; Kopyra, J.; Illenberger, E. *J. Am. Chem. Soc.* **2007**, *129*, 6269–6277.
- (11) Baccarelli, I.; Grandi, A.; Gianturco, F. A.; Lucchese, R. R.; Sanna, N. *J. Phys. Chem. B* **2006**, *110*, 26240–26247.
- (12) Gianturco, F. A.; Lucchese, R. R. *J. Chem. Phys.* **2004**, *120*, 7446–7455.
- (13) Anusiewicz, I.; Sobczyk, M.; Berdys-Kochanska, J.; Skurski, P.; Simons, J. *J. Phys. Chem. A* **2005**, *109*, 484–492.
- (14) Chipman, D. M. *J. Chem. Phys.* **2007**, *127*, 194309.
- (15) Lafosse, A.; Bertin, M.; Domaracka, A.; Pliszka, D.; Illenberger, E.; Azria, R. *Phys. Chem. Chem. Phys.* **2006**, *8*, 5564–5568.
- (16) Sedlacko, T.; Balog, R.; Lafosse, A.; Stano, M.; Matejcik, S.; Azria, R.; Illenberger, E. *Phys. Chem. Chem. Phys.* **2005**, *7*, 1277–1282.
- (17) Bennett, C. J.; Kaiser, R. I. *Astrophys. J.* **2007**, *661*, 899–909.
- (18) Bennett, C. J.; Kaiser, R. I. *Astrophys. J.* **2007**, *660*, 1289–1295.
- (19) Bennett, C. J.; Chen, S. H.; Sun, B. J.; Chang, A. H. H.; Kaiser, R. I. *Astrophys. J.* **2007**, *660*, 1588–1608.
- (20) Bennett, C. J.; Jamieson, C. S.; Osamura, Y.; Kaiser, R. I. *Astrophys. J.* **2006**, *653*, 792–811.
- (21) Bennett, C. J.; Kaiser, R. I. *Astrophys. J.* **2005**, *635*, 1362–1369.
- (22) Holtom, P. D.; Bennett, C. J.; Osamura, Y.; Mason, N. J.; Kaiser, R. I. *Astrophys. J.* **2005**, *626*, 940–952.
- (23) Wada, A.; Mochizuki, N.; Hiraoka, K. *Astrophys. J.* **2006**, *644*, 300–306.
- (24) Cobut, V.; Frongillo, Y.; Patau, J. P.; Goulet, T.; Fraser, M. J.; Jay-Gerin, J. P. *Radiat. Phys. Chem.* **1998**, *51*, 229–243.
- (25) Basch, H.; Hoz, S. *Chem. Phys. Lett.* **1998**, *294*, 117–125.
- (26) Kemnitz, C. R.; Loewen, M. J. *J. Am. Chem. Soc.* **2007**, *129*, 2521–2528.
- (27) Rubin, R. H.; Swenson, G. W.; Benson, R. C.; Tigelaar, H. L.; Flygare, W. H. *Astrophys. J.* **1971**, *169*, L39–L44.
- (28) Hollis, J. M.; Lovas, F. J.; Remijan, A. J.; Jewell, P. R.; Ilyushin, V. V.; Kleiner, I. *Astrophys. J.* **2006**, *643*, L25–L28.
- (29) Nummelin, A.; Bergman, P.; Hjalmarson, A.; Friberg, P.; Irvine, W. M.; Millar, T. J.; Ohishi, M.; Saito, S. *Astrophys. J. Suppl. Ser.* **2000**, *128*, 213–243.
- (30) Schilke, P.; Groesbeck, T. D.; Blake, G. A.; Phillips, T. G. *Astrophys. J., Suppl. Ser.* **1997**, *108*, 301–337.
- (31) Raunier, S.; Chiavassa, T.; Duvernay, F.; Borget, F.; Aycard, J. P.; Dartois, E.; d'Hendecourt, L. *Astron. Astrophys.* **2004**, *416*, 165–169.
- (32) Bockelee-Morvan, D.; et al. *Astron. Astrophys.* **2000**, *353*, 1101–1114.
- (33) Senanayake, S. D.; Idriss, H. *Proc. Natl. Acad. Sci. U.S.A.* **2006**, *103*, 1194–1198.
- (34) Costanzo, G.; Saladino, R.; Crestini, C.; Ciciriello, F.; Di Mauro, E. *BMC Evol. Biol.* **2007**, *7*, S1.
- (35) Cloutier, P.; Sicard-Roselli, C.; Escher, E.; Sanche, L. *J. Phys. Chem. B* **2007**, *111*, 1620–1624.
- (36) Brucato, J. R.; Baratta, G. A.; Strazzulla, G. *Astron. Astrophys.* **2006**, *455*, 395–399.
- (37) Baccarelli, I.; Gianturco, F. A.; Grandi, A.; Lucchese, R. R.; Sanna, N. Electron-driven molecular processes induced in biological systems by electromagnetic and other ionizing sources. In *Advances in Quantum Chemistry*; Elsevier: 2007; Vol. 52, pp 189–230.
- (38) Gianturco, F. A.; Jain, A. *Phys. Rep.* **1986**, *143*, 347–425.
- (39) Lucchese, R. R.; Gianturco, F. A. *Int. Rev. Phys. Chem.* **1996**, *15*, 429–466.
- (40) Hara, S. *J. Phys. Soc. Jpn.* **1967**, *22*, 710–&.
- (41) Perdew, J. P.; Zunger, A. *Phys. Rev. B* **1981**, *23*, 5048–5079.
- (42) Frisch, M. J. et al. *Gaussian 03, Revision C.02*; Gaussian, Inc.: Wallingford, CT, 2004.
- (43) Lucchese, R. R.; Sanna, N.; Natalense, A. P. P.; Gianturco, F. A. ePolyScat (Version E2). [www.chem.tamu.edu/rgroup/lucchese/ePolyScat.E2.manual/manual.html](http://www.chem.tamu.edu/rgroup/lucchese/ePolyScat.E2.manual/manual.html) (accessed May 1, 2008).
- (44) Seydou, M.; Modelli, A.; Lucas, B.; Konate, K.; Desfrancois, C.; Schermann, J. P. *Eur. Phys. J. D* **2005**, *35*, 199–205.

CT800379H